1 Introduction

Fluids, in principle, experience density variation due to temperature changes. This density variation results in a body force on the fluid due to gravity, known as buoyancy. Convection occurs when these forces overcome the fluid's viscosity, resulting in the so-called natural convection.

Convection can be initiated by applying an electric field in a temperature-varying environment. Thermo-Electrohydrodynamic (TEHD) convection studies the behaviour of a differentially heated fluid under the influence of an electric field. Similarly to density, the permittivity of matter changes with temperature. An uneven distribution of permittivity in a fluid under an electric field behaves similarly to natural convection, causing electric-driven convection. Adjusting the electric potential allows control of the amount of forcing from the electrical field.
Brandenburg University of Technology (BTU) conducted GeoFlow I and GeoFlow II experiments to study Earth's mantle and core convection. The experiments involved using two concentric, differentially heated spheres with an applied electric potential to create a radially oriented electric field, which mimicked a planet's gravitational force and triggered convection in the direction of the electric field.
Both experiments were conducted on the International Space Station (ISS). The research focused on TEHD-triggered convection, excluding natural convection, which requires microgravity conditions on the ISS. Additionally, the concentric shells rotate on a turning table, such that both spheres rotate simultaneously, which is known as solid-body rotation. This applied centrifugal and Coriolis forces on the system similar to a planet.

The AtmoFlow experiment, GeoFlow's legacy, brings similar capabilities. It uses an electric field to induce a radial force on the fluid, with expanded parameters for the electric potential and rotation compared to the GeoFlow experiment. The AtmoFlow experiment is conducted on a rotating table, as visible in Figure 1.1(a) to investigate solid-body rotation, and the inner shell is placed on an independently rotating shaft (see

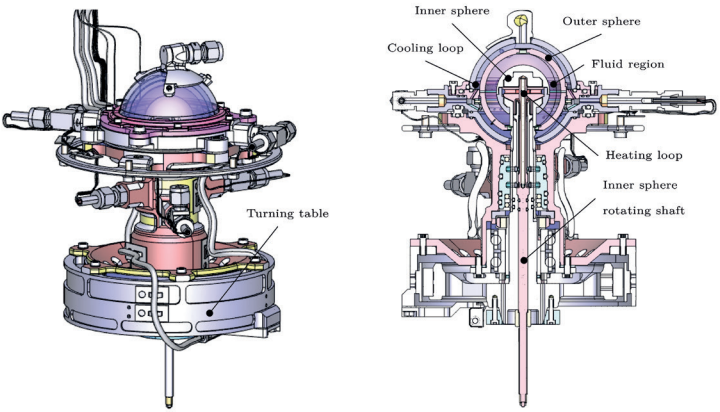

(a) (b)

Figure 1.1.: CAD model of the flight model for the ISS operation of the AtmoFlow experiment in (a) isometric and (b) side cut view, designed and built by Airbus Defense and Space(figures provided by Airbus, funding from DLR via BMWK grant No. 50WP2209).

Figure 1.1(b)), enabling the study of both differential rotation and TEHD convective flows.

The thermal convection pattern is analysed using Wollaston-Schlieren-Interferometry (WSI) [1], where a laser beam is directed through the fluid region and reflected on the inner shell of the experiment. Variations in temperature cause differences in the refractive index along the beam, leading to interference patterns [2] that are captured using a visual recording device. This data is then used to deduce convective patterns in the field.

The method is preferred over other methods like Particle Image Velocimetry (PIV) because of the ISS's strict safety requirements. The particles in the fluid necessary for PIV can alter dielectric fluid properties, leading to voltage breakthrough, potential experiment damage, fire, or toxic fumes.

Composition of the fluid cell

The fluid cell in Figure 1.2 consists of several parts to fulfil the experiment's demands. A steel sphere is positioned in the centre and heated using a heating loop in the equatorial region, applying a temperature gap ΔT to the reference temperature T_0. The steel guarantees good heat conduction from the loop and reflects the laser beam, which is necessary for the WSI. Next is the fluid gap region, also the Region of Interest (RoI). A glass sphere seals the gap, allowing the laser beam to pass through. The top and bottom of the glass sphere are milled to create space for copper inserts. The fluid is continuously pumped around the first glass sphere at the reference temperature. Because copper has higher thermal conductivity, the Poles appear colder to the fluid in the RoI than the glass sphere. A second glass sphere encapsulates this cooling loop. This experiment's heterogeneous temperature boundary condition intends to trigger flow patterns in combination with the differential rotation.

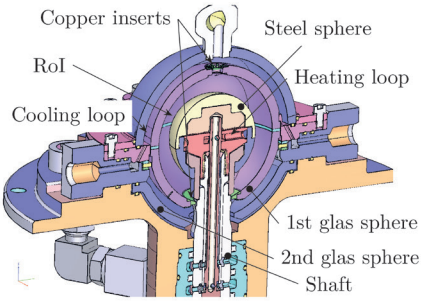

Figure 1.2.: Schematics of the AtmoFlow experiment's fluid cell (figure provided by Airbus, funding from DLR via BMWK grant No. 50WP2209).

The entire setup, including the interferometry system, is placed on a turntable (see Figure 1.1(a)), which is designed to rotate up to 2 Hz. Hence, the experiment occurs in a rotating reference frame. Differential rotation is acquired by turning the inner steel sphere, which is placed on the shaft, up to 2 Hz.
An electric field sets in the gap region. This is achieved using an alternating current source with frequency $f = 1 \cdot 10^4$ Hz connected to the experiment shells. The potential reaches up to 10 kV. Because the inner sphere is made of steel, it is electrically conductive and best suited for building an electric potential on the fluid. However, the sink for the potential, the first glass sphere, is made of glass and hence not electrically conductive. Therefore, a conductive coating is necessary to ensure the sustainability of the electric

Table 1.1.: Geometries and boundaries capabilities of the AtmoFlow experiment

Property	Symbol	Value
Inner radius of RoI (steel sphere)	R_1	18.9 mm
Outer radius of RoI (1st glass sphere)	R_2	27.0 mm
Reference temperature	T_0	293 K
Temperature gap range	ΔT	0-20 K
Steel sphere speed range	Ω_1	$0 - 2$ Hz
Turntable rotation speed range	Ω_2	$0 - 2$ Hz
Electric potential range	V	± 10 kV
Voltage frequency range	f	10 kHz

field. The AtmoFlow's fluid cell geometries and boundary capabilities are summarised in Table 1.1.

1.1 Motivation

The investigation of rotating fluids has a long history. Understanding the physics behind the flow opens new applications for engineering, geophysics, and astrophysics. The pioneer experiment started with the rotation of cylindrical geometries, resulting in Taylor-Couette (TC) flows [3]. The setup consists of two concentric cylinders with a fluid in between. The nature of this setup remains stable until a threshold, and can be described analytically for the stable regime. A cylinder's stable creeping flow depends only on the radial component. Beyond stability, the flow is three-dimensional and needs additional analysis methods. This stability persists due to the evenly distributed angular momentum along the rotating cylinder until the Taylor vortex establishes a new stability level.

The spherical Taylor-Couette (sTC) flow is always three-dimensional due to the curvature of concentric spherical shells, which results in different levels of angular momentum along the meridional component. This imbalance leads to a primary flow in the radial direction in the equatorial region and a secondary flow in the meridional direction that separates at the inner or outer shell to conserve continuity. The choice of rotation speed, whether the inner shell rotates faster or slower than the outer one, can result in different flow configurations, ranging from steady-state flow to transient periodic or turbulent flow.
In spherical TEHD convection, the force vector is mainly in the radial direction and remains stable initially. However, it destabilises after reaching the onset, resembling natural convection. A transient solution sets in by further increasing the force from the

electric field on the fluid. This becomes even turbulent by further increasing it.

The AtmoFlow experiment investigates the combined effects of these mechanisms on flow stability. The campaign focuses on the impact of TEHD convection on the stability of a co-rotating sTC, transitioning from stable parameters to periodic transient and irregular flow. This helps to determine the destabilising or stabilising effect of TEHD convection on sTC.

1.2 Aims and objectives

This thesis investigates the effect of TEHD convection in a spherical gap. The study extends this investigation by independently rotating the shell, creating differential rotation. The aim is to analyse the impact of this combined forcing. The various forces and their interactions result in different flow patterns, profiles, and magnitudes. These variations simultaneously lead to varying levels of heat flux, which depend on the concurrent flow patterns. Based on these findings, the intention is to classify the regimes using diagrams.
The method of information extraction in the ISS experiment is the WSI, which is limited to a temperature gradient. When resolving the interference fringes in time, a velocity deduction is possible. However, this requires an existing thermal convection pattern in the RoI. Tracing it over time provides a rough indication of velocity. Steady-state regimes do not have a moving pattern in the interferogram and, therefore, cannot return velocity information. Retrieving heat flux information from the experiment is also limited. An estimation is possible using the thermal differences in the experiment's heating or cooling loops. However, this returns an integral value but cannot return local phenomena. The aim is to obtain more detailed information regarding velocity and heat transport in the overall gap width.

This work conducts an investigation using Computational Fluid Dynamics (CFD), providing detailed results and refining the parameter space for the ISS onboard experiment. The OpenFOAM engineering toolbox is well-suited since it allows simple implementation of custom equations and post-processing routines.
The experiment built by Airbus is a setup with numerous parts, as shown in Figure 1.1. The boundary condition of the temperature of the fluid spreads through conduction from the heating and cooling loop. Therefore, the boundary condition on the fluid is a Neumann boundary condition, requiring a simulation that includes the solid part around the fluid region. The OpenFOAM CFD software allows this so-called multi-

region simulation. However, the additional complexity makes it much more challenging to interpret the result and associate a specific regime with a given temperature gap or set electric potential.
Current work processes an idealised model with Dirichlet temperature boundary conditions that link the dimensionless numbers directly to a resulting regime. This model simplifies the origin of the resulting flow patterns and heat flux, allowing for a more accurate analysis of the kinetic energy and its correlation with the heat flux. It also explores the transition from stable to transient and irregular flows. The investigation does not account for the influence of centrifugal buoyancy or dielectric heating, which restricts the number of parameters and provides a more accurate conclusion regarding the origin of the flow state, the resulting heat flux, and flow patterns.
The equations in this work are solved dimensionless, and the forcing parameters are lumped into dimensionless parameters. In a numerical model, the range for those dimensional parameters is endless. However, this investigation stays within the experiment's capabilities. The fluid in use boils at high temperatures and also has a breakdown voltage. Hence, the temperature and voltage parameters lumped in the dimensionless numbers must fulfil AmtoFlow's capabilities seen in Table 1.1.
The parameters for sTC range from viscous to periodic transient cases. The maximum rotation rate is determined when the flow from TEHD convection becomes marginal compared to the induced convection from rotation. This initial step provides preliminary parameters of interest for the upcoming AtmoFlow campaign on the ISS. Since the parameters for the ISS experiments are limited, this work simultaneously offers a priority classification for the onboard experiment.
To summarise, the focus of retrieved information is therefore set to:

- Resulting temperature and velocity profile for qualitative pattern analysis
- Quantitative analysis of heat flux from inner to outer shell
- Investigation about conductive and convective heat and the associated kinetic energy
- Propose a resulting regime diagram based on the competing pattern from sTC flow and the TEHD convection

1.3 Outline

The thesis is structured in nine chapters. An appendix provides further details about derivation and verification. After the introduction, the following sections are written:

- **Fundamentals and theory**: This section details the governing equations necessary to understand the modelling employed. It also explains the procedure for obtaining dimensionless equations and the resulting dimensionless numbers, representing the forcing parameters for the computed cases.

- **The current state of research**: The past research about TEHD convection and differential rotation is summarised in the named section. Each forcing and resulting flow of the literature is chronologically named, and the quintessence of each paper is briefly stated.

- **Computational and numerical modelling**: This chapter outlines transitioning from the physical experiment to the numerical model. It provides a detailed description of the simplified geometry and boundary conditions. Additionally, it includes information about the choice of solver and its settings, as well as evidence supporting mesh independence. Furthermore, due to limited computational time and the need to save only a reasonable amount of data, the capabilities of the AtmoFlow parameters must be selected. The methods used for selecting the processed parameters are explained. Finally, the chapter outlines the diagnostics necessary to achieve the aims previously mentioned.

- **TEHD convection in spherical shell**: Before stepping into the combination of differential rotation and TEHD convection flows, this section investigates the basic state of TEHD convection simulation with isothermal boundary conditions. The results presented are an extension of the existing GeoFlow experiments, and the differences from the current work are discussed.

- **Non-isothermal spherical Taylor-Couette flow**: Analogously, the differential rotation flow is investigated. The blend from steady-state to transient simulations of the selected parameter is shown and discussed for these simulations. This section, in particular, highlights the non-linear behaviour of differential rotation, which makes scalability challenging. Furthermore, the impact of the chosen aspect ratio on the margin of transient cases is shown.

- **TEHD convection in spherical Taylor-Couette flow with meridional isothermal boundary conditions**: After analysing the forcing independently, this chapter investigates the results by combining TEHD convection with differential rotation in a spherical system. The temperature boundaries remain isothermal for the processed case, and the new resulting patterns are compared to the isolated forcing from the prior chapter. Ultimately, a regime diagram is proposed.

- **TEHD convection in spherical Taylor-Couette flow with experiment-like thermal boundary conditions**: This chapter changes the isothermal temperature boundary condition to more experiment-like boundary conditions from the AtmoFlow experiment. The results are processed similarly to prior outcomes, compared and discussed.
- **Conclusion and outlook**: The last chapter summarises the knowledge gained from this thesis and proposes an outlook for future work.

2 Fundamentals and theory

This chapter introduces the fundamentals and theory of the governing equations to solve sTC flows and TEHD convection. It begins with the equations related to electric fields and the resulting force on fluids, followed by a description of the continuity and motion equations. The section then covers the transport of heat and concludes with the process of non-dimensionalising these equations.

2.1 Fluids under electric fields

The current section introduces the resulting force and heat generation from an electric field on a fluid. The focus is on dielectric fluids, and the sections explain the Kortweg-Helmholtz force density to a dielectric fluid and simplify Maxwell's equations.

2.1.1 Fluid properties

The effect of an electric field on a given fluid depends significantly on the molecular structure and charge of the fluid's composition. Fluids with free charges, like ions, see them moving within the fluid, generating an electric current. For a direct current (DC) source, those ions deposit on the cathode or the anode, depending on their charge. The moving charges between the ions cause ohmic heat, and if the current becomes significant, electromagnetism also needs to be considered [4]. An alternating current (AC) source with a high enough frequency can maintain those free charges in place, as

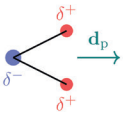

Figure 2.1.: Schematic of a polar molecule and its dipole $\mathbf{d}_\mathrm{p}$.

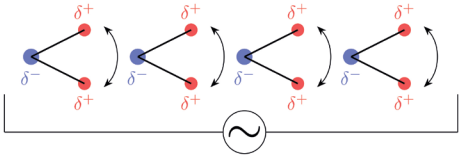

Figure 2.2.: Schematic of the source of dielectric heating from a high-frequency AC source on polar molecules.

their acceleration is not strong enough to follow the change of direction of the electrical field.

Dielectric fluids do not have free-moving charges by definition, but they can be polar. In the presence of an electric field, they orient according to the direction of the electric field and their dipole $\mathbf{d}_\mathrm{p}$ as schematically shown in Figure 2.1.

For the DC source, the molecules remain stationary. The non-polar module sees its dipole shift according to the source but remains stationary. Suppose an AC source is applied to a dielectric fluid composed of polar molecules, schematically shown in Figure 2.2. The molecules oscillate according to the source frequency. If the frequency becomes high enough, the friction on the molecular level becomes significant enough to generate measurable heat. This phenomenon is called dielectric heating.

2.1.2 Force resulting from an electric field on a dielectric fluid

The electric field $\mathbf{E}$ resulting in a force on a dielectric fluid is derived by the Kortweg-Helmholtz force density $\mathbf{f_E}$ described by Landau and Lifshitz [5] and written as

$$\mathbf{f_E} = \rho_\mathrm{e}\mathbf{E} + \boldsymbol{\nabla}\left[\rho\left(\frac{\partial\epsilon}{\partial\rho}\right)_T \frac{\mathbf{E}^2}{2}\right] - \frac{1}{2}\mathbf{E}^2\boldsymbol{\nabla}\epsilon \tag{2.1}$$

where ρ_e is the electric charge density, ϵ the permittivity and ρ the density. $\boldsymbol{\nabla}$ describes the nabla operator.

The first term

$$\mathbf{f}_\mathrm{EP} = \rho_\mathrm{e}\mathbf{E} \tag{2.2}$$

in the eq. (2.1) represents the electrophoretic (EP) force, which arises from the interaction of the moving free charges in the fluid within the electric field $\mathbf{E}$. This force is significant in cases where static or low-frequency electric fields are being studied. The